8π-periodic dissipationless ac Josephson effect on a quantum spin Hall edge via a quantum magnetic impurity

Hoi-Yin Hui* and Jay D. Sau

Department of Physics, Condensed Matter Theory Center and Joint Quantum Institute, University of Maryland, College Park, Maryland 20742-4111, USA

(Received 18 October 2016; published 9 January 2017)

Time-reversal invariance places strong constraints on the properties of the quantum spin Hall edge. One such restriction is the inevitability of dissipation in a Josephson junction between two superconductors formed on such an edge without the presence of interaction. Interactions and spin-conservation breaking are key ingredients for the realization of the dissipationless ac Josephson effect on such quantum spin Hall edges. We present a simple quantum impurity model that allows us to create a dissipationless fractional Josephson effect on a quantum spin Hall edge. We then use this model to substantiate a general argument that shows that any such nondissipative Josephson effect must necessarily be 8π periodic.

DOI: 10.1103/PhysRevB.95.014505

I. INTRODUCTION

The Josephson effect [1–3], which was originally a direct manifestation of macroscopic quantum coherence in superconductors, has turned out to be one of the most reliable ways of diagnosing the topological properties of a junction. Topological superconductors (TSCs) supporting Majorana modes have been shown to demonstrate a 4π-periodic Josephson effect [4–10], which is doubled period compared with the conventional Josephson effect. This phenomenon, which is known as the fractional Josephson effect, has been observed in quite a few devices [11,12] including the quantum spin Hall edge [13,14]. At first this is quite counterintuitive given that the Hamiltonian itself is 2π periodic. The fractional Josephson effect in this case arises because the topological property of the superconductor forces the local fermion parity (FP) of the junction to change with each rotation of the phase by 2π. If one assumes contact with a bath that equilibrates the system to the ground state of the appropriate FP [15] then the topological nature of the superconductor is precisely reflected in the fractional Josephson effect. Interestingly, the addition of interaction can often modify the topological classification qualitatively [16,17]. In fact, some of the states such as parafermion states in superconductors [18] are already known to be characterized by exotic Josephson effects.

While several topological superconducting phases involving interactions have been proposed [18–20], not many of them are within experimental reach. On the other hand, an interesting 8π-periodic Josephson effect, which relies on the combination of interaction and topology that has recently been proposed [21] certainly appears to be within the realm of experimental possibility. Ideally, one could just obtain this effect by studying a Josephson junction (JJ) on an interacting two-dimensional topological insulator (TI) edge [21].

However, as we discuss in this paper, the 8π Josephson effect turns out to be the only possible nondissipative Josephson effect that a quantum spin Hall edge can support. To understand what we mean by nondissipative Josephson effect consider a finite-voltage-biased Josephson junction as is used to study the ac Josephson effect. The ideal response of such a Josephson junction to a voltage bias is to create an ac current that can be measured as radiation. However, at large finite voltages, a typical Josephson junction dissipates part of its energy through processes that generate quasiparticles in the bulk [22]. The dissipation in turn leads to a dc current in addition to the ac current, which is parametrized by the shunt resistance of the junction. In this paper, we will be interested in understanding the conditions under which such effect shunt resistances can be avoided in TI junctions.

As we review in more detail later, even though a noninteracting TI edge with a ferromagnetic insulator (FI) is predicted to have a 4π-periodic fractional Josephson effect [6,7], removing the FI qualitatively modifies this effect. In the absence of a relaxation mechanism or for a short junction, the JJ on the TI edge has a 2π periodicity characteristic of conventional Josephson junctions. The dissipation, which is observable as a parallel shunt resistance across the junction [22], arises here from ejection of quasiparticles into the conduction band. The addition of a relaxation mechanism also leads to a dissipative but 4π-periodic fractional Josephson effect [15]. Thus, one can say that the Josephson effect on a noninteracting TI edge with time-reversal symmetry (TRS) is always dissipative and fundamentally accompanied by a shunt resistance. As shown by Zhang and Kane [21], the addition of interaction qualitatively changes this story and introduces a topologically protected 8π-periodic fractional Josephson effect, which is nondissipative (i.e., free of the shunt resistance). It is worth noting that this effect, unlike the 4π-, 8π-, and 12π-periodic Josephson effect that can arise from fine-tuning in conventional systems [23], is indeed topologically protected in the sense that it is completely robust against all perturbations of the Hamiltonian that preserve time-reversal symmetry.

In this paper, we study the effect of a strongly interacting quantum dot (QD) in a quantum spin Hall Josephson junction. By considering a simple model of such a QD that acts like a spin coupled to Andreev bound states (ABSs) [24], we show that such a junction would show an 8π-periodic fractional Josephson effect, in contrast with the 4π periodicity expected from time-reversal breaking topological junction. We then argue that the generic low voltage periodicity of the quantum

*Present Address: Department of Physics, Virginia Tech, Blacksburg, Virginia 24061, USA.

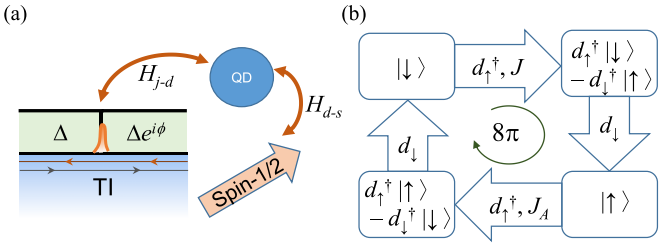

FIG. 1. (a) The system with a short Josephson junction whose Andreev state is tunnel coupled to a quantum dot. The quantum dot is coupled to another localized spin [Eq. (1)]. (b) Schematic diagram showing the 8π cycle of states. $|\uparrow,\downarrow\rangle$ represent the states of the spin and $d^\dagger_{\uparrow,\downarrow}$ represents the electron in the quantum dot. J, J_A represents the spin-symmetric and -asymmetric exchange interactions inside the dot, respectively. In each 2π cycle of phase shown by the bold arrow a spin-up electron is pumped into or a spin-down hole leaves the edge.

spin Hall Josephson junction is 8π as opposed to the 4π periodicity for time-reversal-breaking topological junctions. In fact, while higher frequencies could lead to 2π- or 4π-periodic Josephson effects, such ac Josephson effects are necessarily dissipative, i.e., accompanied by a finite dc current.

II. JUNCTION WITH A QUANTUM DOT

While the nondissipative 8π-periodic Josephson effect is generic, we start by demonstrating its origin through the simple device shown in [Fig. 1(a)]. This model incorporates the key ingredients for a nondissipative Josephson effect; namely, a topological quantum spin Hall edge, spin-conservation breaking, and interaction. The device in [Fig. 1(a)] consists of a JJ on a quantum spin Hall (QSH) edge laterally coupled to a strongly interacting multi-orbital quantum dot. The interaction is chosen to be large enough so that the quantum dot admits at most two electrons. Furthermore, the Hund's coupling is also assumed to be strong so that one of the levels is always occupied by one electron, which can thus be considered to be a local moment with spin $\mathbf{S}$. The resulting spin $-1/2$ is exchanged coupled to the dot electron with spin $\mathbf{s}$ via the Hund's coupling through a Hamiltonian

$$H_{d-s} = J\boldsymbol{S}\cdot\boldsymbol{s} + J_A(S^+s^+ + S^-s^-) + \varepsilon_d(d_\uparrow^\dagger d_\uparrow + d_\downarrow^\dagger d_\downarrow), \tag{1}$$

where the spin of the dot electron $d^\dagger_{\sigma=\uparrow,\downarrow}$ can be written as $\boldsymbol{s} = \frac{1}{2}\sum_{\alpha\beta} d_\alpha^\dagger \boldsymbol{\sigma}_{\alpha\beta} d_\beta$. In addition, a projection constraint ensures no double occupancy of the electron level $d_\sigma^\dagger$. The term proportional to J is the Heisenberg interaction between the dot and the spin, while J_A represents the process in which spin conservation is broken.

The QD with Hamiltonian Eq. (1) is tunnel coupled to the QSH edge [25] through a Hamiltonian [26,27]

$$H_{j-d} = t[a_\uparrow^\dagger(x=0)d_\uparrow + a_\downarrow^\dagger(x=0)d_\downarrow + \text{H.c.}], \tag{2}$$

where $a_\sigma^\dagger(x=0)$ creates electrons on the QSH edge. A time-reversal-breaking impurity on the QSH edge is expected to produce a 4π-periodic Josephson effect because of the flip of fermion parity with each 2π shift of the phase ϕ. While the spin in the QD acts as a magnetic impurity, as illustrated in Fig. 1(b), this only works in the case of odd fermion parity of the JJ where, by the Kramers theorem, the ground state is twofold degenerate. As will be shown, while the QD returns to an odd-FP state each 4π period (as in the time-reversal-breaking case), the spin in the QD is flipped over each such period. This leads to the generic 8π periodicity of the current as a function of phase.

To quantitatively illustrate the mechanism in Fig. 1(b), we consider the limit of weak tunnel coupling t, the quantum dot electron can only tunnel to a low-energy ABS in a Josephson junction on the edge written as $\gamma^\dagger = \sum_\sigma \int dx(u_\sigma a_\sigma^\dagger + v_\sigma a_\sigma)$ with an energy $E(\phi)$, which depends on the phase difference across the Josephson junction. The effective Hamiltonian of the edge ABS is written as

$$H_j = E(\phi)(\gamma^\dagger\gamma - 1/2). \tag{3}$$

The wave function of the ABS γ and its energy are solved from the Bogoliubov–de Gennes (BdG) Hamiltonian of the JJ:

$$\mathcal{H}_{\text{BdG}} = \tau_z(-iv_F s_z\partial_x - \mu) + \Delta\cos\phi(x)\tau_x + \Delta\sin\phi(x)\tau_y, \tag{4}$$

where s and τ are Pauli matrices on spin and Nambu spaces, respectively, and $\phi(x) = \phi\theta(x)$. Since $[\mathcal{H}_{\text{BdG}}, s_z] = 0$, the solutions are labeled with the eigenvalues of s_z, where the solution with $s_z = +1$ have $E(\phi) = -\Delta\cos\frac{\phi}{2}$, $u_\uparrow(x=0) = v_\downarrow(x=0)^* = \sqrt{\sin(\phi/2)/(2\xi)}e^{-i\phi/4}$, and $u_\downarrow = v_\uparrow = 0$ in the interval $0 \leqslant \phi \leqslant 2\pi$, while its particle-hole-conjugated partner is the other branch of solution with $s_z = -1$. With this explicit form of quasiparticle solution, we can therefore rewrite H_{j-d} as

$$H_{j-d} = t(u_\uparrow d_\uparrow^\dagger\gamma + v_\downarrow\gamma d_\downarrow + \text{H.c.}), \tag{5}$$

where we have dropped the position arguments of $u_\uparrow$ and $v_\downarrow$.

The simplified form of the effective coupling allows us to describe the cycle of the QD shown in Fig. 1(b) as the phase ϕ is varied. During each cycle of advancing ϕ by 2π forward, a quasiparticle is "pumped" from the bulk occupied states towards the conduction states through the edge states. The excitation of a bulk conduction-band electron must be avoided to prevent dissipation. This can be accomplished by adding a spin-up electron or removing a spin-down electron from the QD (and releasing a Cooper pair). Starting with the state $|\downarrow\rangle$ at $\phi = 0$, i.e., with the dot empty and localized spin at $S_z = -1$. During an increment of 2π of ϕ, a spin-up electron is added to the dot from the bulk, which due to the hybridization term Eq. (1) forms a singlet with the localized spin $(d_\uparrow^\dagger|\uparrow\rangle - d_\downarrow^\dagger|\downarrow\rangle)/\sqrt{2}$. In the next cycle a spin-down electron is removed from the dot, leaving the localized spin at $S_z = +1(|\uparrow\rangle)$. The electron leaving the dot can combine with the next electron coming from the bulk and exit as a Cooper pair. The next two cycles proceed similarly, with J_A breaking spin conservation to result in a triplet state after the third cycle $(d_\uparrow^\dagger|\uparrow\rangle - d_\downarrow^\dagger|\downarrow\rangle)/\sqrt{2}$ and returning to the original state $|\downarrow\rangle$ at $\phi = 8\pi$.

The above process can be put on quantitative footing by projecting the Hamiltonian into the low-energy Hilbert space and solving for the energy-phase relation (EΦR), as detailed in Appendix A. Typical results with J_A being zero or nonzero

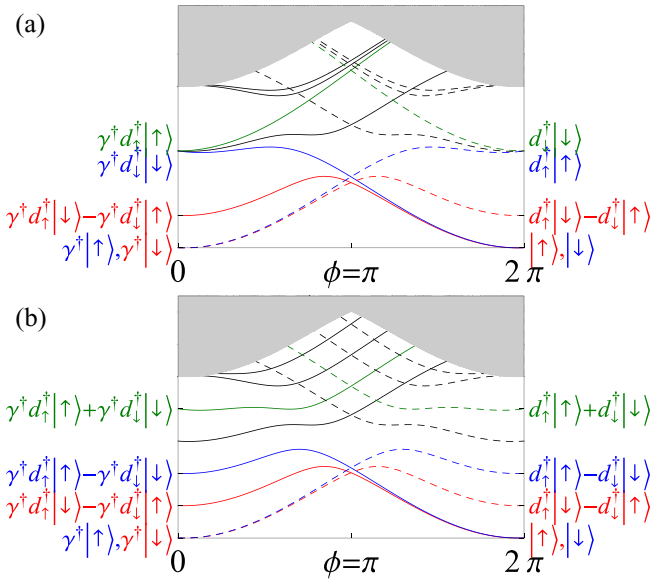

FIG. 2. The (many-electron) energy spectrum of a coupled SC junction/QD/spin system [Eqs. (1)–(3)] as a function of superconducting phase ϕ with $J = 0.2\Delta$ and $\varepsilon_d = 0.5\Delta$ and (a) $J_A = 0$ (spin-conserving case) and (b) $J_A = J$ (spin-anisotropic case). The solid lines represent odd total fermion parity (Kramers degenerate) states and the dashed lines represent even total fermion parity states. The fermion parity changes with each 2π cycle of ϕ and the color represents the curves corresponding to various eigenstates. Following the spectrum in panel (a) we find that the ground state necessarily couples to the bulk states. In the spin-conservation breaking in panel (b), the spectrum is isolated from the bulk states and 8π periodic.

are shown respectively in Figs. 2(a) and 2(b). In the absence of the term proportional to J_A, the full 8π cycle could not be completed nondissipatively because the dot-spin triplet state could not be formed. Figure 2(a) illustrates that the state is eventually driven into the continuum, thereby dissipating away the Josephson current. Alternatively, dissipation of the excess energy into a phonon might lead to a dissipative 4π-periodic process. With nonzero J_A [Fig. 2(b)], a full cycle of states fully gapped from other excited states can be obtained. We also note that J_A breaks spin conservation along the z direction. The connection of the absence of spin conservation with the prevention of dissipation will be elaborated below.

III. CONDITIONS FOR DISSIPATIONLESS JOSEPHSON EFFECT

We now discuss in general the necessary conditions to realize a topological TRS Josephson junction without dissipation. We first review how this is accomplished in the case where time-reversal symmetry is broken by a FI element in a topological junction with only one ABS [see Fig. 3(a)]. The EΦR is shown in Fig. 3(c). At $\phi \neq 2\pi p$, where p is an integer, a particle-hole pair of ABS is present in the junction. Without the FI which breaks TRS, these states are required to join the continuum modes ($|E| = \Delta$) at the time-reversal-invariant points $\phi = 2\pi p$ in order to satisfy the Kramers theorem (black lines). This requirement corresponds [see Fig. 3(d)] to the adiabatic change of the phase ϕ connecting the ground

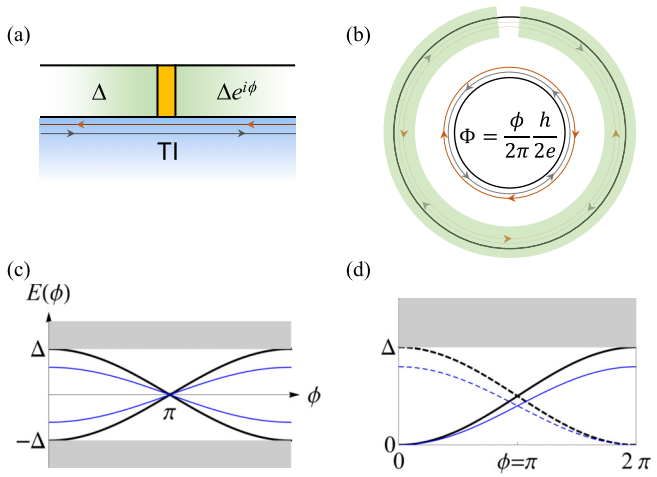

FIG. 3. (a) A short Josephson junction on a one-dimensional TI edge. (b) Equivalent construction where now the phase difference is controlled by threading a flux through the center of the Corbino disk. (c) The single-particle Andreev spectrum for the junction with (blue thin lines) or without (black thick lines) the FI element. (d) The many-body EΦR with (blue thin lines) or without (black thick lines) the FI element, where solid (dotted) lines indicate states with even (odd) parity.

state at $\phi = 0$ with the continuum at $\phi = 2\pi$. This creates quasiparticle excitations in the bulk that lead to dissipation in the Josephson junction. On the other hand, with the FI that breaks TRS even at $\phi = 2\pi p$, the ABSs remain disconnected from the continuum modes [blue lines in Fig. 3(c)], and thus the many-body state remains gapped from the continuum [blue lines in Fig. 3(d)]. The full 4π cycle of Josephson current could then be completed without dissipation if the temperature and rate of change of ϕ are low enough.

As seen in Fig. 4(a), the ABS levels in the noninteracting case connect the valence bands to the conduction bands [6]. This is a necessary consequence of the Kramers degeneracy and the time-reversal (i.e., $\phi \to -\phi$) properties of the eigenvalues shown in Fig. 4(a). This leads us to conclude

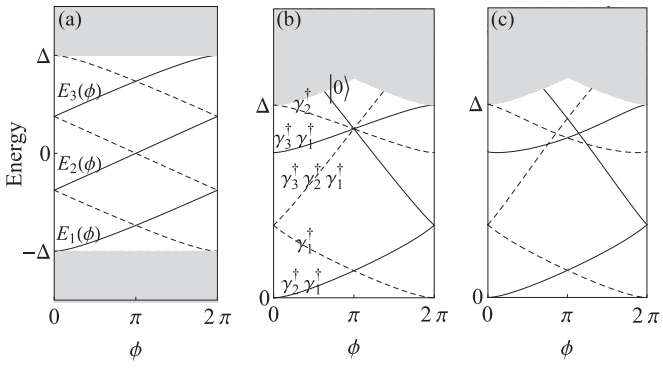

FIG. 4. (a) EΦR for a junction with length $L = \pi v_F/\Delta_0$. The solid (dotted) lines are solutions with eigenvalues $s_z = \pm 1$ (b) Many-body spectrum for the same noninteracting junction. Black (dotted) lines are states with even (odd) parity. The labels indicate which of the ABSs are occupied. (c) Many-body spectrum for a junction with s_z-conserving interactions. Detailed calculations are presented in Appendix B.

that interactions are necessary to avoid dissipation in TRS topological Josephson junctions. Next we argue that spin-conservation breaking is crucial to avoid dissipation in the TI Josephson junction. To understand this, consider a Josephson junction built from a Corbino geometry [shown in Fig. 3(b)], in which the phase difference ϕ between the two sides of the junction is controlled by threading a flux $\Phi_{\text{flux}} = \frac{\phi}{2\pi}\Phi_0$ through the center of the setup, where $\Phi_0 = \frac{h}{2e}$ is the SC flux quantum. For the sake of the argument, we first take out the SC and FI elements, leaving behind a Corbino disk made of TI. It is known that, if spin is conserved along the polarization axis of the TI, the system exhibits quantized spin Hall conductance and, by Laughlin's argument [28], threading a flux quantum has the effect of pumping a pair of spins with $s_z = \pm 1$ to opposite edges. This effect still holds with the introduction of SC, since s-wave superconductivity preserves s_z conservation. In this scenario, the portion of the TI edge not in contact with the SC can provide a finite number of ABSs (say, n_A) to accommodate the pumped spins. After threading n_A SC flux quanta (corresponding to an incrementation of ϕ by $2\pi n_A$), the ABSs fail to accommodate *all* of the pumped spins, leading to the occupation of the other continuum modes on the edges, which corresponds to a dissipation in the Josephson junction. The way to avoid this is to break s_z conservation, which would then destroy the quantized spin Hall conductance of the system. Threading a flux quantum would then flip the fermion parities (FPs) of the two edges [6].

Based on these two observations, we expect that a dissipationless Josephson junction in a TI requires an interaction term that breaks s_z conservation to a junction. This agrees with what we found in the Josephson junction coupled with a quantum dot as described above, where the term J_A provides the necessary breaking of spin conservation, without which dissipation could not be avoided.

IV. ROLE OF SPIN ANISOTROPY

To gain further insight into the necessity of breaking spin conservation to obtain a dissipationless TRS topological junction, we look into another example, first studied in Ref. [21]. Consider a SC-N-SC junction on a TI edge where the normal (N) portion is long enough with multiple ABSs present. The Hamiltonian is almost identical to our previous example [Eq. (4)] except that Δ is chosen to represent a long junction as $\Delta(x) = \Delta_0\theta(|x| - \frac{L}{2})$. When $L = \pi v_F/\Delta$, three ABSs are present for all values of ϕ, and the single-particle and many-body EΦR are shown in Figs. 4(a) and 4(b), respectively. The key feature in Fig. 4(b), which is needed to understand the Josephson behavior, is the fourfold degeneracy at $\phi = \pi$. As discussed in Ref. [21], splitting this degeneracy by Coulomb interactions into two twofold Kramers degenerate crossings. However, as seen in Fig. 4(c), the states still continue to reach the continuum in the absence of spin-conservation-breaking interactions. This forbids a dissipationless ac Josephson effect in this case. To understand this, we note that the four states have different number of quasiparticles: $\{|0\rangle, \gamma_2^\dagger|0\rangle, \gamma_3^\dagger\gamma_1^\dagger|0\rangle, \gamma_3^\dagger\gamma_2^\dagger\gamma_1^\dagger|0\rangle\}$, and therefore have different values of s_z. Once the fourfold degeneracy is lifted we are left with twofold degeneracies at level crossings. These crossings are, however, between states of different s_z. In accordance with our general arguments presented above, we find that s_z-conserving interaction terms [e.g., $\int dx(a_\uparrow^\dagger a_\uparrow + a_\downarrow^\dagger a_\downarrow)^2$] in the Hamiltonian cannot split these crossings and the ground state necessarily reaches the continuum simply by adiabatic evolution. Adding s_z-breaking interactions such as $\int dx(a_\uparrow^\dagger a_\uparrow a_\downarrow^\dagger \partial_x a_\uparrow - a_\downarrow^\dagger a_\downarrow a_\uparrow^\dagger \partial_x a_\downarrow) + \text{H.c.}$, which were assumed to be comparable to the Coulomb interactions in Ref. [21], are required to split the crossings to avoid dissipation.

V. GENERAL THEOREM FOR 8π PERIODICITY

The two examples of dissipationless TRS topological junctions above both exhibit 8π periodicities. We now argue that this is directly a consequence of TRS present in the junction. To see this, consider a TRS junction described locally by the Hamiltonian $H(\phi)$ where ϕ is the phase difference of the constituent SCs. This Hamiltonian satisfies

$$H(\phi) = H(\phi + 2\pi) = \Theta H(-\phi)\Theta^{-1}, \tag{6}$$

where the first condition follows from the 2π periodicity of the phase of SC. The second condition, where Θ is the time-reversal operator, follows from the time-reversal of the magnetic flux that creates the superconducting phase ϕ. Let us suppose that $|n\rangle_\phi$ is the nth excited many-body state at phase ϕ satisfying $H(\phi)|n\rangle_\phi = E_n(\phi)|n\rangle_\phi$ and $FP|n\rangle_\phi = \lambda_n(\phi)|n\rangle_\phi$, where FP is the fermion parity operator and E_n and λ_n are, respectively, its energy and FP eigenvalues with $\lambda_n(\phi) = \pm 1$ when there are even or odd number of fermions in the system, respectively. It then follows from Eq. (6) that

$$E_n(\phi) = E_n(\phi + 2\pi) = E_n(-\phi). \tag{7}$$

Finally, we stipulate that the FP must switch as ϕ is advanced by 2π, i.e.,

$$\lambda_n(\phi + 2\pi) = -\lambda_n(\phi), \tag{8}$$

which describes the topological property of the TI. More specifically, threading a flux through the TI Corbino disk [see Fig. 3(b)] changes the Z_2 "time-reversal polarization" [29], which can be identified with the FP of each of the edges [6]. We remark that this property is not captured by the local Hamiltonian (6) of the junction.

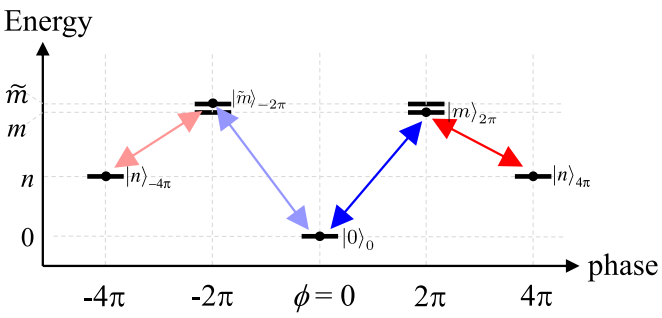

FIG. 5. The path of an adiabatically followed even-parity state. Blue (red) and light blue (light red) lines are time-reversed paths of each other. The crucial point is $n \neq 0$, because otherwise $|0\rangle_0$ would join to $|\tilde{m}\rangle_{2\pi}$ and $|m\rangle_{2\pi}$ simultaneously.

The proof of 8π periodicity for a state with even FP is illustrated in Fig. 5, and the mathematically rigorous proof is given in the Appendix C. Let us start with a nondegenerate state $|0\rangle_0$. Tuning ϕ forward and backward by 2π reaches the degenerate states $|m\rangle_{2\pi}$ and $|\tilde{m}\rangle_{-2\pi}$ [recall that, by Eq. (8), $|m\rangle_0$ and $|\tilde{m}\rangle_0$ are odd-parity states and is a Kramers pair at $\phi = 0$]. Further increasing or decreasing ϕ by 2π, the state $|n\rangle_{\pm 4\pi}$ is reached. From Eq. (7) we know that $|n\rangle_{4\pi} \neq |0\rangle_0$ because $|0\rangle_0$ cannot be adiabatically connected to both $|m\rangle_{2\pi}$ and $|\tilde{m}\rangle_{2\pi}$ at the same time (compare, e.g., light red and deep blue lines in Fig. 5). The proof for a state with odd FP proceeds in a similar way and is discussed in the appendix.

In summary, interactions and spin-conservation breaking are the two key ingredients that are required to permit a dissipationless ac Josephson effect in a TRS topological Josephson junction. In this paper, we have given a general proof that the EΦR of such a dissipationless TRS topological Josephson junction is 8π periodic in ϕ. The 8π periodicity arises from the combination of the flip of FP and spin over each 2π period. We have shown that these ingredients can be incorporated naturally in a model of a quantum dot coupled to a Josephson junction on a TI edge.

Note added. During the preparation of the manuscript we became aware of a related recently published work by Peng *et al.* [30].

ACKNOWLEDGMENTS

This work is supported by JQI-NSF-PFC and the University of Maryland startup grant. H.H. acknowledges support from AFOSR (FA9550-15-1-0445) and ARO (W911NF-16-1-0182) during the final stage of this work. We acknowledge the discussion with Carlo Beenakker.

APPENDIX A: LOW-ENERGY HAMILTONIAN FOR THE JUNCTION-DOT SYSTEM

Since the Hamiltonian (1) conserves the parity of electron number, we expand it in odd- and even-parity subspaces. We also take the limit $U \to \infty$, which projects out the states where the quantum dot is doubly occupied. The basis states for the odd-parity subspace are $\{\gamma^\dagger|\uparrow\rangle, \gamma^\dagger|\downarrow\rangle, d_\uparrow^\dagger|\downarrow\rangle, d_\downarrow^\dagger|\uparrow\rangle, d_\uparrow^\dagger|\uparrow\rangle, d_\downarrow^\dagger|\downarrow\rangle\}$, where $|\uparrow/\downarrow\rangle$ satisfies $S^z|\uparrow/\downarrow\rangle = \pm|\uparrow/\downarrow\rangle$ and $\gamma|\uparrow/\downarrow\rangle = d_\sigma|\uparrow/\downarrow\rangle = 0$. The Hamiltonian in this basis is

$$H^{(o)} = \begin{pmatrix} \frac{E(\phi)}{2} & 0 & 0 & 0 & tu_\uparrow^* & 0 \\ 0 & \frac{E(\phi)}{2} & tu_\uparrow^* & 0 & 0 & 0 \\ 0 & tu_\uparrow & -\frac{E(\phi)}{2} - \frac{J}{2} + \varepsilon_d & J & 0 & 0 \\ 0 & 0 & J & -\frac{E(\phi)}{2} - \frac{J}{2} + \varepsilon_d & 0 & 0 \\ tu_\uparrow & 0 & 0 & 0 & -\frac{E(\phi)}{2} + \frac{J}{2} + \varepsilon_d & J_A \\ 0 & 0 & 0 & 0 & J_A & -\frac{E(\phi)}{2} + \frac{J}{2} + \varepsilon_d \end{pmatrix}, \tag{A1}$$

while in the even subspace with basis $\{|\uparrow\rangle, |\downarrow\rangle, \gamma^\dagger d_\uparrow^\dagger|\downarrow\rangle, \gamma^\dagger d_\downarrow^\dagger|\uparrow\rangle, \gamma^\dagger d_\uparrow^\dagger|\uparrow\rangle, \gamma^\dagger d_\downarrow^\dagger|\downarrow\rangle\}$, the Hamiltonian is expanded as

$$H^{(e)} = \begin{pmatrix} -\frac{E(\phi)}{2} & 0 & 0 & -tv_\downarrow & 0 & 0 \\ 0 & -\frac{E(\phi)}{2} & 0 & 0 & 0 & -tv_\downarrow \\ 0 & 0 & \frac{E(\phi)}{2} - \frac{J}{2} + \varepsilon_d & J & 0 & 0 \\ -tv_\downarrow^* & 0 & J & \frac{E(\phi)}{2} - \frac{J}{2} + \varepsilon_d & 0 & 0 \\ 0 & 0 & 0 & 0 & \frac{E(\phi)}{2} + \frac{J}{2} + \varepsilon_d & J_A \\ 0 & -tv_\downarrow^* & 0 & 0 & J_A & \frac{E(\phi)}{2} + \frac{J}{2} + \varepsilon_d \end{pmatrix}. \tag{A2}$$

Finally, we note that at $\phi = 2n\pi$, $v_\downarrow = u_\uparrow = 0$ which enables us to reach the simple forms of eigenstates shown in Figs. 1(c) and 1(d).

APPENDIX B: BOGOLIUBOV–DE GENNES SOLUTION FOR A LONG TOPOLOGICAL JUNCTION

Since s_z commutes with $\mathcal{H}_{\rm BdG}$, the solutions to $\mathcal{H}_{\rm BdG}\psi_n = E_n\psi_n$ are labeled by the "spin" index $s_z = \pm 1$. The $s_z = +1$ solutions, denoted by $\psi_n^{(+)}$, have $u_{n\downarrow}^{(+)} = v_{n\uparrow}^{(+)} = 0$ and

$$u_{n\uparrow}^{(+)} = \mathcal{A}_n e^{{\rm sgn}(x) i\theta_{E_n}/2} \exp\left[i\frac{\phi(x)}{2} + i\bar{\mu}\bar{x} - \sqrt{1-\bar{E}_n^2}\left||\bar{x}| - \frac{\bar{L}}{2}\right|\right], \tag{B1a}$$

$$v_{n\downarrow}^{(+)} = \mathcal{A}_n e^{-{\rm sgn}(x) i\theta_{E_n}/2} \exp\left[-i\frac{\phi(x)}{2} + i\bar{\mu}\bar{x} - \sqrt{1-\bar{E}_n^2}\left||\bar{x}| - \frac{\bar{L}}{2}\right|\right], \tag{B1b}$$

for $|x| > \frac{L}{2}$, and

$$u_{n\uparrow}^{(+)} = \mathcal{A}_n e^{-i\theta_{E_n}/2} \exp\left[i\bar{\mu}\bar{x} + i\bar{E}_n\left(\bar{x} + \frac{\bar{L}}{2}\right)\right], \tag{B1c}$$

$$v_{n\downarrow}^{(+)} = \mathcal{A}_n e^{i\theta_{E_n}/2} \exp\left[i\bar{\mu}\bar{x} - i\bar{E}_n\left(\bar{x} + \frac{\bar{L}}{2}\right)\right], \tag{B1d}$$

otherwise. Here the normalization factor is $\mathcal{A}_n = [2L + 2\xi/(1-\bar{E}_n^2)^{1/2}]^{-1/2}$, and $\bar{E} = \frac{E}{\Delta_0}$, $\bar{\mu} = \frac{\mu}{\Delta_0}$, $\bar{x} = \frac{x}{\xi} = \frac{x}{v_F/\Delta_0}$, $\bar{L} = \frac{L}{\xi}$, $e^{\pm i\theta_{E_n}} = \bar{E}_n \pm i(1-\bar{E}_n^2)^{1/2}$, where $\bar{E}_n$ satisfies

$$\sqrt{1-\left(\frac{E_n}{\Delta_0}\right)^2}\cos\left(\frac{E_n L}{v_F}-\frac{\phi}{2}\right) - \frac{E_n}{\Delta_0}\sin\left(\frac{E_n L}{v_F}-\frac{\phi}{2}\right) = 0. \tag{B2}$$

The $s_z = -1$ solutions $\psi_n^{(-)}$ with energy $-E_n$ are related to $\psi_n^{(+)}$ by particle-hole conjugation, $\psi_n^{(-)} = \Xi\psi_n^{(+)}$, where $\Xi = s_y\tau_y K$. With the solutions to $\mathcal{H}_{\text{BdG}}$ we can expand the Hamiltonian in quasiparticle operators as

$$H_0(\phi) = \sum_n E_n(\phi)\left(\gamma_n^\dagger\gamma_n - \frac{1}{2}\right), \tag{B3}$$

where E_n are determined from Eq. (B2) and $\gamma_n^\dagger = \sum_{\sigma=\uparrow/\downarrow}\int dx(u_{n\sigma}^{(+)}a_\sigma^\dagger + v_{n\sigma}^{(+)}a_\sigma)$. Since only the branch of solutions with $s_z = +1$ are summed, the number of quasiparticles in a many-body state coincide with the value of s_z for that state.

APPENDIX C: MATHEMATICALLY RIGOROUS PROOF OF 8π PERIODICITY

Let $U_{\phi_2,\phi_1} = \exp[-i\int_{\phi_1}^{\phi_2} H(\phi)d\phi]$ be the operator that adiabatically changes the phase from ϕ_1 to ϕ_2. The conditions

$$|m\rangle_{\phi_2} = U_{\phi_2,\phi_1}|n\rangle_{\phi_1} \Leftrightarrow |n\rangle_{\phi_1} = U_{\phi_1,\phi_2}|m\rangle_{\phi_2} \tag{C1a}$$

$$\Leftrightarrow |m\rangle_{2p\pi+\phi_2} = U_{2p\pi+\phi_2,2p\pi+\phi_1}|n\rangle_{2p\pi+\phi_1}, \tag{C1b}$$

for all integers p follows directly from the unitarity of U and Eq. (7).

We first consider the case where the ground state at $\phi = 0$, $|0\rangle_0$, has even FP, i.e., $\lambda_0(0) = 1$ (Fig. 5). Starting with $|0\rangle_0$, as the phase is adiabatically tuned to 2π and 4π, the state is brought to the mth and nth excited states, respectively, i.e.,

$$U_{2\pi,0}|0\rangle_0 = |m\rangle_{2\pi}, \tag{C2a}$$

$$U_{4\pi,2\pi}|m\rangle_{2\pi} = |n\rangle_{4\pi}. \tag{C2b}$$

Now we know $m \neq 0$ because, from Eqs. (8), $\lambda_0(2\pi) = -\lambda_0(0) = -1$, i.e., the FP of the ground state at $\phi = 2\pi$ is odd. The state that $|0\rangle_0$ transforms into must be even in FP, i.e., $\lambda_m(2\pi) = \lambda_0(0) = 1$, and from Eq. (8) we have $\lambda_m(0) = -1$, i.e., $|m\rangle_0$ is odd in FP. Since $H(0)$ is TRS, the Kramers theorem guarantees that there is an orthogonal state $|\tilde{m}\rangle_0 = \Theta|m\rangle_0$ with the same energy: $E_{\tilde{m}}(0) = E_m(0)$. Apply Θ to Eqs. (C2) we have

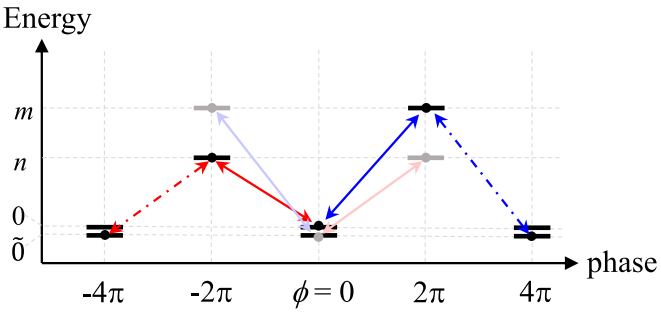

FIG. 6. For an odd-parity state we define m and n as the states that Kramers pair $\{|0_0\rangle, |\tilde{0}_0\rangle\}$ traverses as a flux quantum is inserted in either direction. Here again, deep-colored and light-colored lines are time-reversed paths of each other. Use Eq. (7) to shift the light blue and light red lines by 4π, we get the dashed path, completing the full 8π-periodic path that the state follows.

$$U_{-2\pi,0}|0\rangle_0 = |\tilde{m}\rangle_{-2\pi}, \tag{C3a}$$

$$U_{-4\pi,-2\pi}|\tilde{m}\rangle_{-2\pi} = |n\rangle_{-4\pi}. \tag{C3b}$$

We have thus obtained an energy-phase relation (EΦR) schematically shown in Fig. 5 which is 8π periodic *if* $n \neq 0$ (and assuming no accidental degeneracy $E_n \neq E_0$). To establish this, we use Eq. (C1) to derive from Eq. (C3b)

$$U_{2\pi,0}|n\rangle_0 = |\tilde{m}\rangle_{2\pi}, \tag{C4}$$

which can be compared with Eq. (C2a). Since $U_{0,2\pi}|m\rangle_{2\pi} = |0\rangle_0$, we know $U_{0,2\pi}|\tilde{m}\rangle_{2\pi} \neq |0\rangle_0$ (as $|0\rangle_0$ cannot be adiabatically connected to two states at $\phi = 2\pi$) and from Eq. (C4) this means $n \neq 0$. The 8π-periodic EΦR is therefore established.

The case of $\lambda_0(0) = -1$ can be considered in a similar fashion (Fig. 6). Let $|0\rangle_0$ and $|\tilde{0}\rangle_0$ be the Kramers pair of degenerate ground states at $\phi = 0$. Define $|m\rangle_{2\pi}$ and $|n\rangle_{-2\pi}$ be, respectively, the states that $|0\rangle_0$ transforms into as ϕ is tuned from 0 to $\pm 2\pi$, respectively. We have

$$U_{2\pi,0}|0\rangle_0 = |m\rangle_{2\pi}, \quad U_{-2\pi,0}|0\rangle_0 = |n\rangle_{-2\pi}, \tag{C5}$$

$$U_{2\pi,4\pi}|\tilde{0}\rangle_{4\pi} = |m\rangle_{2\pi}, \quad U_{-2\pi,-4\pi}|\tilde{0}\rangle_{-4\pi} = |n\rangle_{-2\pi}, \tag{C6}$$

where the second line is obtained by applying Θ and Eq. (C1b) subsequently on the first line. Finally, we use Eq. (C1b) to derive, from the last relation above,

$$U_{2\pi,0}|\tilde{0}\rangle_0 = |n\rangle_{2\pi}. \tag{C7}$$

Upon comparison with the first relation of Eq. (C5), this shows that $n \neq m$ and hence the full 8π-periodic cycle of EΦR shown in Fig. 6 (with $E_n \neq E_m$) is established.

[1] B. D. Josephson, Rev. Mod. Phys. **36**, 216 (1964).
[2] I. O. Kulik, Low Temp. Phys. **36**, 841 (2010).
[3] A. A. Golubov, M. Y. Kupriyanov, and E. Il'ichev, Rev. Mod. Phys. **76**, 411 (2004).
[4] A. Y. Kitaev, Phys. Usp. **44**, 131 (2001).
[5] H.-J. Kwon, K. Sengupta, and V. M. Yakovenko, Eur. Phys. J. B **37**, 349 (2004).
[6] L. Fu and C. L. Kane, Phys. Rev. B **79**, 161408 (2009).

[7] Y. Tanaka, T. Yokoyama, and N. Nagaosa, Phys. Rev. Lett. **103**, 107002 (2009).
[8] R. M. Lutchyn, J. D. Sau, and S. Das Sarma, Phys. Rev. Lett. **105**, 077001 (2010).
[9] Y. Oreg, G. Refael, and F. von Oppen, Phys. Rev. Lett. **105**, 177002 (2010).
[10] D. M. Badiane, M. Houzet, and J. S. Meyer, Phys. Rev. Lett. **107**, 177002 (2011).
[11] L. P. Rokhinson, X. Liu, and J. K. Furdyna, Nat. Phys. **8**, 795 (2012).
[12] D. J. van Woerkom, A. Proutski, B. van Heck, D. Bouman, J. I. Väyrynen, L. I. Glazman, P. Krogstrup, J. Nygård, L. P. Kouwenhoven, and A. Geresdi, arXiv:1609.00333.
[13] J. Wiedenmann, E. Bocquillon, R. S. Deacon, S. Hartinger, O. Herrmann, T. M. Klapwijk, L. Maier, C. Ames, C. Brüne, C. Gould, A. Oiwa, K. Ishibashi, S. Tarucha, H. Buhmann, and L. W. Molenkamp, Nat. Commun. **7**, 10303 (2016).
[14] R. S. Deacon, J. Wiedenmann, E. Bocquillon, T. M. Klapwijk, P. Leubner, C. Brüne, S. Tarucha, K. Ishibashi, H. Buhmann, and L. W. Molenkamp, arXiv:1603.09611.
[15] C. W. J. Beenakker, D. I. Pikulin, T. Hyart, H. Schomerus, and J. P. Dahlhaus, Phys. Rev. Lett. **110**, 017003 (2013).
[16] L. Fidkowski and A. Kitaev, Phys. Rev. B **81**, 134509 (2010).
[17] E. Tang and X.-G. Wen, Phys. Rev. Lett. **109**, 096403 (2012).
[18] R. S. Mong, D. J. Clarke, J. Alicea, N. H. Lindner, P. Fendley, C. Nayak, Y. Oreg, A. Stern, E. Berg, K. Shtengel *et al.*, Phys. Rev. X **4**, 011036 (2014).
[19] Y. Oreg, E. Sela, and A. Stern, Phys. Rev. B **89**, 115402 (2014).
[20] E. Gaidamauskas, J. Paaske, and K. Flensberg, Phys. Rev. Lett. **112**, 126402 (2014).
[21] F. Zhang and C. L. Kane, Phys. Rev. Lett. **113**, 036401 (2014).
[22] D. Averin and A. Bardas, Phys. Rev. Lett. **75**, 1831 (1995).
[23] B. Sothmann, J. Li, and M. Büttiker, New J. Phys. **15**, 085018 (2013).
[24] N. M. Chtchelkatchev and Y. V. Nazarov, Phys. Rev. Lett. **90**, 226806 (2003).
[25] B. L. Altshuler, I. L. Aleiner, and V. I. Yudson, Phys. Rev. Lett. **111**, 086401 (2013).
[26] J. I. Väyrynen, M. Goldstein, and L. I. Glazman, Phys. Rev. Lett. **110**, 216402 (2013).
[27] J. I. Väyrynen, M. Goldstein, Y. Gefen, and L. I. Glazman, Phys. Rev. B **90**, 115309 (2014).
[28] R. B. Laughlin, Phys. Rev. B **23**, 5632 (1981).
[29] L. Fu and C. L. Kane, Phys. Rev. B **74**, 195312 (2006).
[30] Y. Peng, Y. Vinkler-Aviv, P. W. Brouwer, L. I. Glazman, and F. von Oppen, Phys. Rev. Lett. **117**, 267001 (2016).